STM JOURNALS

Journal of
Remote Sensing & GIS

https://journals.stmjournals.com/jorsg

ISSN: 2230-7990 (Online)
ISSN: 2321-421X (Print)
Volume 16, Issue 1, 2025
January–April
DOI (Journal): 10.37591/JoRSG

Research JoRSG

Role of Satellite Data Assimilation on ERA-Interim and ERA5 Wave Parameter Ratios: A Case Study Based on Year-Long In-Situ Observations in the Bay of Bengal

M. Kalyani[1,*], K. Ramesh[2], B. Kesava Kumar[1], P. Murugesh[1], K. Jossia Joseph[3], M. Arul Muthiah[3]

Abstract

The rapid decline in energy resources forced mankind to tap other forms of natural energy resources in the light of an exponential increase in demand due to overpopulation. The energy from ocean waves is one of the cleanest sources of energy available perennially that changes seasonally and is site-specific. To assess the wave power potential at any site, knowledge of wave parameters such as wave height, period, and direction is necessary. In-situ moored buoy measurements are confined to only a few strategic locations, whereas satellite-derived wave parameters are subjected to the satellite pass, periodicity, and suffer representation errors and boundary effects. Hence, numerical models are necessary which provide gridded data globally. The model improvement is accorded by calibration, validation, and data assimilation of observations as ground truth. In the present study, two of the European Centre for Medium-Range Weather Forecasts (ECMWF) global reanalysis (satellite data assimilated) products viz., ERA-Interim and ERA5 are taken into consideration to assess their performance against the moored buoy measurements at a deepwater location (83.27°E/13.99°N) on the Northwest Bay of Bengal during 2005 utilizing a year-long measurement covering pre-monsoon, monsoon, and post-monsoon seasons. This location is under the influence of local forcing as wind waves and remote forcing in the form of swells coming from the Southern Indian Ocean, monsoons as well as cyclones. Various aspects that governed the effectiveness of ERA5 over ERA-Interim for improving the model prediction are discussed. The site-specific regional constants in the form of wave parameter ratios between the moored buoy observations and ECMWF models (ERA5 and ERA-Interim) are derived for each month accounting for the seasonal variation. The improved estimates with satellite data assimilation aid in the design criteria of wave energy converters, and improved forecast skill during high-intensity cyclones which are on the verge of increase due to climate change impacts.

Keywords: Moored buoy, ERA-Interim, ERA5, significant wave height, peak period, wave parameter ratio

***Author for Correspondence**
M. Kalyani
E-mail: kalyani.niot@gmail.com

[1]Scientist-E, OOS Group, National Institute of Ocean Technology, Chennai, Tamil Nadu, India
[2]Scientific Officer II, OOS Group, National Institute of Ocean Technology, Chennai, Tamil Nadu, India
[3]Scientist-F, OOS Group, National Institute of Ocean Technology, Chennai, Tamil Nadu, India

Received Date: December 05, 2024
Accepted Date: December 09, 2024
Published Date: December 15, 2024

Citation: M. Kalyani, K. Ramesh, B. Kesava Kumar, P. Murugesh, K. Jossia Joseph, M. Arul Muthiah. Role of Satellite Data Assimilation on ERA-Interim and ERA5 Wave Parameter Ratios: A Case Study Based on Year-Long In-Situ Observations in the Bay of Bengal. Journal of Remote Sensing & GIS. 2025; 16(1): 1–20p.

INTRODUCTION

Wave energy assessment in Indian waters is strongly dependent on the seasons and monsoons. Numerical wave models predict the combined wave height of seas from local winds and swells from distant storms to a reasonable accuracy but fail to correctly predict the individual components, more so in the case of remote swells due to various model assumptions. Insufficient wind resolution, linearization, parametrization, and enforcing ease of computational burden in dealing with nonlinear wave-wave interactions; refraining wave models from accurate spectral evolution, thereby affecting the wave period and wave height prediction. This leads to an underestimation of extreme wave heights during cyclones or monsoons compared to observations that are crucial for design purposes. Hence, observations are essential to assess model performance and correct model errors using data assimilation to improve forecasts. Long-term observations are vital for understanding the seasonal and interannual variability of wave characteristics and quantifying model errors in order to evaluate site-specific constants for a chosen numerical model.

The evaluation of sustainable wave power and the maximum wave power are crucial for optimizing the design of wave energy converters in light of the increasing number of cyclones due to climate change. Wave characteristics in Indian waters are essential for estimating the wave power. As observations are scant, wave model data are essential. Therefore, the performance of the wave model must be tested before its utilization. Indian waters are influenced by seasonal variations in the monsoonal winds. As waves are forced by winds, joint analysis of the variability of winds and waves is important and has been studied [1] during 1998–2009. An intercomparison of wind and wave data between ERA-Interim and National Centers for Environmental Prediction (NCEP) Climate Forecast System Reanalysis is presented [2]. The performance of ERA-Interim wave data in nearshore waters around India was evaluated [3]. The surface wave climatology and its variability in the North Indian Ocean were analyzed [4] based on ERA-Interim data. Based on the MIKE 21 spectral wave model hindcast data forced by ERA-Interim winds, the seasonal and interannual changes in significant wave height in shelf seas around India during 1998–2012 were studied [5]. The space and time variations of the maximum wave height were analyzed in detail using 40 years of data from the ERA5 model in the shelf seas of India [6]. The performance of ERA5 (1979–2019) data of significant wave height (sea, swell, and total) proved to be good when validated with calibrated multi-platform satellite altimetry data in the Indian Ocean [7] and reported climatological trends and spatiotemporal variability.

Extensive research has been conducted on wave power resource estimation at regional and global levels. The potential to generate power from waves along the coastline of India was assessed [8]. The potential for energy from local wind waves in India is discussed in detail [9]. The wave energy potential and its harvesting method were assessed [10] along the Indian coast. Spatiotemporal variations in wave energy on the west coast of India have been studied in coastal waters [11]. The global wave energy resource was assessed [12]. A review of the assessment of wave energy resources for best utilization was presented [13].

Wave period characteristics are essential for the design of wave energy converters. The peak period provides a direct clue of where the peak energy is concentrated in the wave spectrum, which can occur either in the wind-sea band or the swell band depending on the relative contributions of seas and swells based on the season during the year. Cahill (2014) [14] described that the wave period ratio varies with spectral shape and location, depending on the sea state, and showed that low sea states with mixed seas exhibit higher ratios. Wave power estimates of the Irish coast were improved by 18% based on the revised wave period ratio for the theoretical Bretschneider and Joint North Sea Sea Wave Project (JONSWAP) spectra [15]. Assimilating satellite altimeter data into the numerical model MFWAM (Météo-France WAve Model) and using the updated wave period ratio improved the average wave power by up to 30% [16] in a region off the northwestern coast of Ireland when compared to using other numerical models such as WWIII without assimilation.

In this study, the impact of satellite data assimilation on the reanalysis products ERA-Interim and ERA5 was assessed and validated using in situ (moored buoy) observations in the NW Bay of Bengal. In addition, regional constants in the form of wave parameter ratios, wave height ratio (WHR), and wave

ISSN: 2230-7990 (Online), ISSN: 2321-421X (Print)

period ratio (WPR) are derived for both significant wave height (Hs) and peak wave period (Tp) for both ERA-Interim and ERA5 and are compared. This study provides the effect of chronological developments and improvements in satellite data assimilation to the reanalysis wave parameter products of the ECMWF, that is, ERA-Interim and ERA5, at a location of interest in the Northwest Bay of Bengal when compared with the moored buoy observations covering the pre-monsoon, monsoon, and post-monsoon seasons during 2005. The correlation and root-mean-square error statistics provided insight into the relative improvement in the performance of the models. Furthermore, the significant wave height (WHR) and peak WPR of each model with respect to moored buoy observations were provided for each month to tap the seasonal variation as well as the variation with respect to the reanalysis products ERA-Interim and ERA5.

DATA

Year-long (2005) wave data of significant wave height (Hs), peak wave period (Tp), and mean wave direction (MWD) at 3 hours intervals obtained from the in-situ measurements of an offshore moored buoy deployed off Machilipatnam (83.27°E/13.99°N) in the Bay of Bengal at 3267 m water depth by the Ocean Observation Systems Group of the National Institute of Ocean Technology (NIOT), Chennai, India, were used in the present study. The NIOT has been maintaining the Indian moored buoy network at strategic locations in the North Indian Ocean for more than 2.5 decades and has provided data on critical met-ocean parameters. These observations are regularly used for (i) calibration to tune the model to observations, (ii) validation to assess model performance, (iii) assimilation to improve forecasting, and (iv) identification of lacuna and improvisation of model physics.

Model Data

In this study, the ECMWF ERA-Interim and ERA5 Reanalysis Wave datasets at the buoy site were used. Reanalysis is a process that combines model data with observations through the state-of-the-art data assimilation system (4DVAR) fed with several years/decades worth of observations, such as altimeter data and ocean boundary conditions, to provide a numerical description of the climate. A highly realistic model based on numerical weather prediction was used to propagate the atmospheric state over time. That state (background) is updated at regular intervals, typically 6 or 12 hours, with observations to form the analysis at that time. This update step uses 4DVAR, whereby the cost function is iteratively minimized. The 4DVAR analysis system was introduced at the ECMWF for operational numerical weather prediction in 1997 [17] in the Integrated Forecasting System (IFS). The atmospheric model also provides constraints (radiation, dynamics, and physics) that help enforce a physically realistic analysis. These constraints also ensure that the analyzed variables are consistent with one another [18]. This reconstruction of the weather over the entire globe (for global reanalyzes) takes the form of gridded datasets that feature no gaps and consequently attract users outside the specialized weather community. The input for the wave model was provided by the atmospheric model in the form of wind input. Hence, the improvements to the wind datasets of ECMWF products by data assimilation/reanalysis are directly reflected in the wave model improvement. Reanalysis wave data are now widely used in wave climate studies on global and regional scales [2, 4].

ECMWF Reanalysis Products

The ERA5 and ERA-Interim Wave Datasets (Hs, Tp, MWD) for the year 2005 were utilized in this study. Their performance was evaluated with respect to moored buoy data from the buoy site in 2005. ERA5 is a fifth-generation atmospheric reanalysis produced by the European Centre for Medium-Range Weather Forecasts (ECMWF). It provides hourly estimates of numerous atmospheric, land, and oceanic climate variables from 1940 onwards, covering the Earth on a 31-km horizontal grid and resolving the atmosphere with 137 levels from the surface up to a height of 80 km. This state-of-the-art global dataset was freely available from the Climate Data Store of the Copernicus Climate Change Service (https://cds.climate.copernicus.eu/#!/home). Chronological details of the ECMWF reanalysis are presented in Table 1. The characteristics of the ERA-5 and ERA-Interim reanalysis products are detailed in Table 2.

Table 1. The chronological details of ECMWF reanalysis [24].

Reanalysis	Period covered	Grid resolution	Assimilation scheme	IFS model cycle (year)	Reference
Atmospheric reanalyzes					
FGGE	1979	208 km	OI	(1980)	*[19]*
ERA-15	1979–1994	125 km	OI	13r4 (1995)	[20]
ERA-40	1957–2002	125 km	3D-Var	23r4 (2001)	[21]
ERA-Interim	1979–2019	80 km	4D-Var	31r2 (2006)	*[22]*
ERA5	1950–present	31 km	4D-Var	41r2 (2016)	*[23]*

Source: From Hersbach et al. (2020) [24]

Table 2. Characteristics of ERA5 and ERA-Interim reanalyzes [24].

	ERA5	ERA-Interim
Characteristics		
Implementation date	8 March 2016	12 December 2006
Horizontal resolution	T_L 636 (~31 km)	T_L 255 (~79 km)
Horizontal transform grid	0.3° × 0.3°	0.75° x 0.75°
Vertical resolution	137 levels up to 0.01 hPa	60 levels up to 0.1 hPa
Temporal resolution	1-hourly	6-hourly
IFS cycle	41r2	31r2
Period covered	1950-present	1979–2019
Reference	[24]	[22]

METHODOLOGY

The time-series data of Hs, Tp, and MWD at 3-hour intervals at the buoy location during 2005 were utilized for the analysis. The corresponding model wave parameters of Hs, Tp, and MWD are extracted from ERA-Interim (using the ERA-Interim archive, API code) (Latitude 0.75°N, Longitude 0.75°E and at 6-hourly intervals) and ERA5 (Latitude 0.5°N, Longitude 0.5°E and at 3-hourly intervals) (*https://cds.climate.copernicus.eu/cdsapp#!/dataset/reanalysis-era5-single-levels?tab=form*) for the year 2005 at the nearest grid to the buoy location based on the space, time resolutions of the global model gridded data sets of ECMWF.

ANALYSIS AND RESULTS

Annual Wave Parameter Variation

The yearly time-series comparison of Hs between the Buoy Observed, ERA5, and ERA-Interim Models is shown in Figure 1. The peak southwest monsoonal waves were underpredicted by both models, with ERA-Interim showing large deviations. The cyclone-induced wave heights during the post-monsoon period are also highly underpredicted by both ERA5 and ERA-Interim, with ERA5 exhibiting improvement over ERA-Interim. The yearly time-series comparison of Tp between the Buoy Observed, ERA5, and ERA-Interim Models is shown in Figure 2.

The time-series of Tp helps to directly understand the origin of the wave activity, either locally or remotely. The variation of Tp from January to mid-February depicts two distinct peaks (double/mixed seas) revealing both local and remote swells from the Southern Indian Ocean (SIO) with total Hs in the range of 0.5 to 1.5 m. March and April are mostly characterized by long-period swells with less local wave activity during summer.

May, a transition from the pre-monsoon to the southwest monsoon exhibits the longest swells during the middle of May with two distinct peaks at the beginning and end of the month at the DS5 Buoy site. June month mostly witnessed local wind wave activity with Hs in the range of 2.0 to 3.5 m. July is characterized by both local seas with monsoonal wave activity and swells from SIO. In August, there was a decrease in the wave heights and mixed waves.

Journal of Remote Sensing & GIS
Volume 16, Issue 1
ISSN: 2230-7990 (Online), ISSN: 2321-421X (Print)

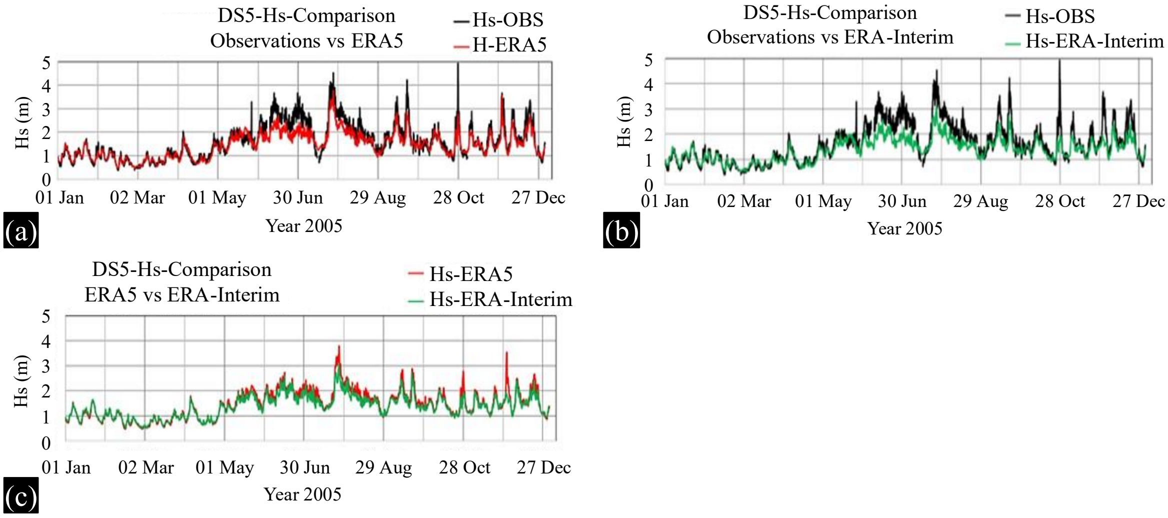

Figure 1. Yearly time-series comparison of Hs; (a) OBS versus ERA5; (b) OBS versus ERA-Interim; and (c) ERA5 versus ERA-Interim data sets.

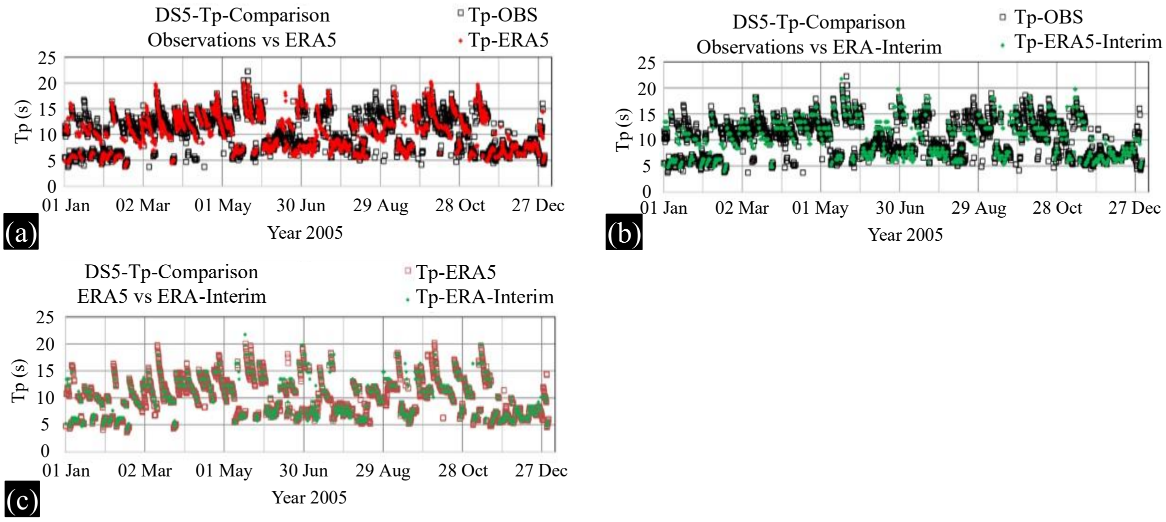

Figure 2. Yearly time-series comparison of Tp; (a) OBS versus ERA5; (b) OBS versus ERA-Interim; and (c) ERA5 versus ERA-Interim data sets.

During the transition (September) to the northeast monsoon, mixed seas were observed with high Hs governed by the cyclone/deep depression. October month is dominated by swells with wave heights reaching a maximum of 2.0 m, except during the cyclone at the end of October which recorded the peak Hs of approximately 5.0 m (Tp between 5 and 10 s) during the year. November and December exhibit Hs in the range of 1.0 to 3.0 m except during cyclone (3.5 m), and is characterized by local wind seas, while mid-November witnessed swells with Hs less than 1.0 m.

Annual Single-Parameter Distribution

The annual Hs, Tp, and MWD distributions under different class intervals as a percentage of occurrence during 2005 are plotted in Figure 3(a)–(c), respectively.

Annual Hs Distribution

Buoy-Hs spanned from 0 to 5.0 m, whereas the ERA5 and ERA-Interim Model Hs spanned from 0 to 3.5 m, 0.5 and 3.0 m, respectively. ERA-Interim exhibited high occurrences in the 1.0 to 2.0 m range and low occurrences for higher waves between 2.0 and 2.5 m compared to ERA5 and Buoy. Buoy-Hs varied in a wider range with the percentage occurrence up to 1.5 m slightly close to ERA5.

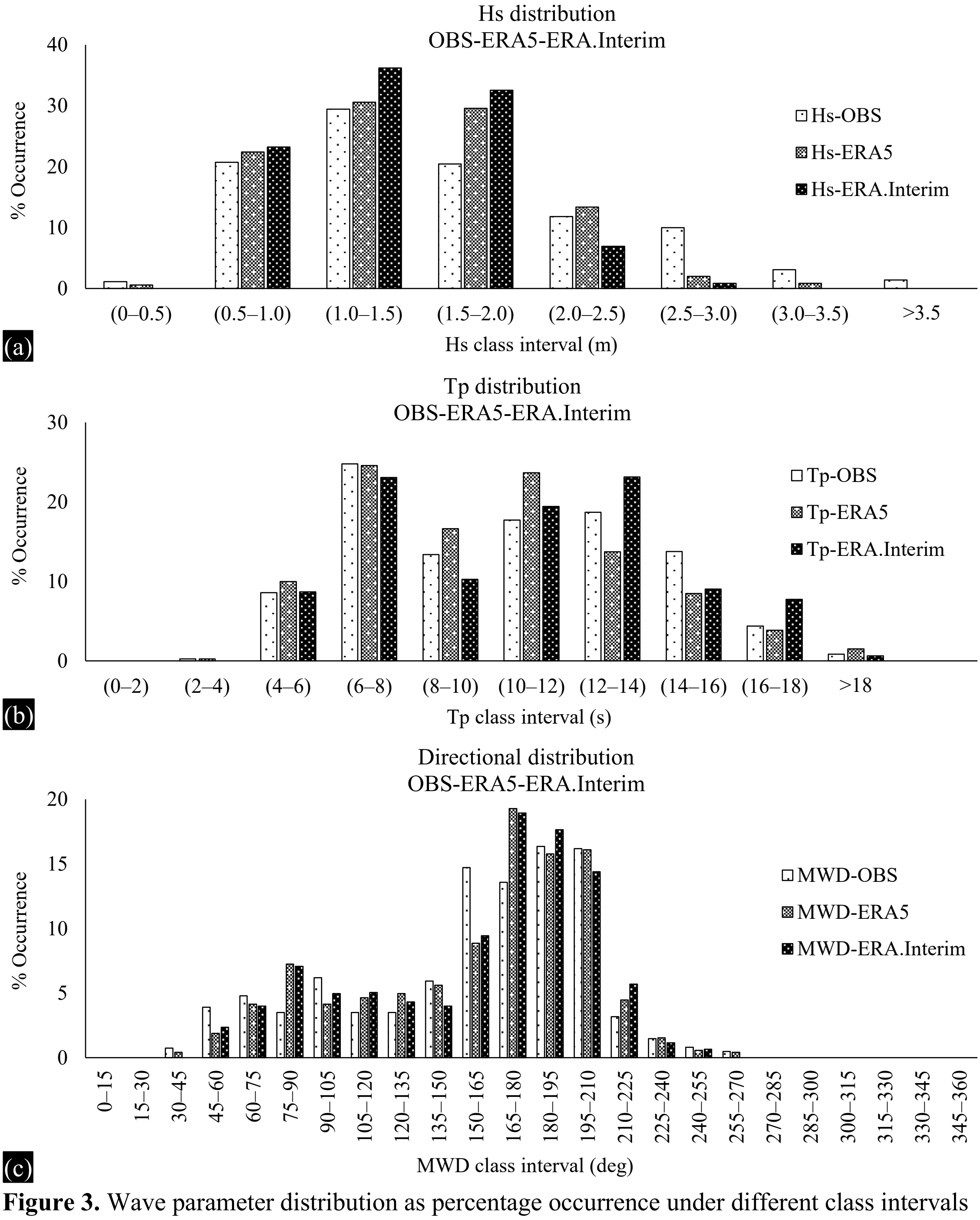

Figure 3. Wave parameter distribution as percentage occurrence under different class intervals during 2005; (a) Hs, (b) Tp, and (c) MWD.

In the intermediate range of 1.5 to 2.0 m, a wide difference is observed between Buoy and ERA5 with Buoy occurrence on the lower side. While the occurrence in the range 2 to 2.5 m is in a similar range, for waves higher beyond 2.5 m, buoy occurrence is greater.

Annual Tp Distribution

The percentage occurrence of ERA-Interim predicted waves with Tp up to 8 s in the wind-sea range is closer to that of the buoy, but slightly on the lower side. In the mixed sea range between Tp 8 s and 12 s, the ERA-Interim deviation was high and underpredicted the occurrence of Tp. In the swell range (Tp>12 s), the occurrence of Tp was highly overestimated. The ERA5 prediction of Tp occurrences in

ISSN: 2230-7990 (Online), ISSN: 2321-421X (Print)

the wind-sea range is more or less similar to that of Buoy, who observed Tp up to 8 s. In the mixed sea range of 8–12 s, ERA5 overpredicted Tp occurrences with high deviations. The occurrence of swell waves with Tp in the range of 12–16 s is highly underpredicted by ERA5. In addition, smaller deviations were observed for ERA5 for much longer swells (>16 s). It is interesting to note that ERA5 and ERA-Interim Tp occurrences with respect to that of the buoy showed an inverse trend. This could be attributed to the poor temporal and spatial resolutions of the ERA-Interim Analysis.

Annual MWD Distribution

The predominant MWD was confined to the sector 150°(SSE)–210°(SSW), with occurrences ranging between 10% and 20%. In the directional sector 45°(NE)–150°(SSE), the occurrence ranged between 3% and 8%. High deviations between the buoy and both models were observed in the sectors 150°–165° (high underestimation) and 165°–80° (high overestimation), respectively. Further, in the sectors, 75°–90° and 210°–225° also both models exhibited an overestimation of occurrences. The rest of the sectors were generally underestimated by the models.

Annual Joint Distribution

Annual Joint Distribution of Hs and MWD

Wave rose diagrams are plotted based on the joint distribution of Hs and MWD using the Buoy, ERA5, and ERA-Interim datasets, and are compared in Figure 4.

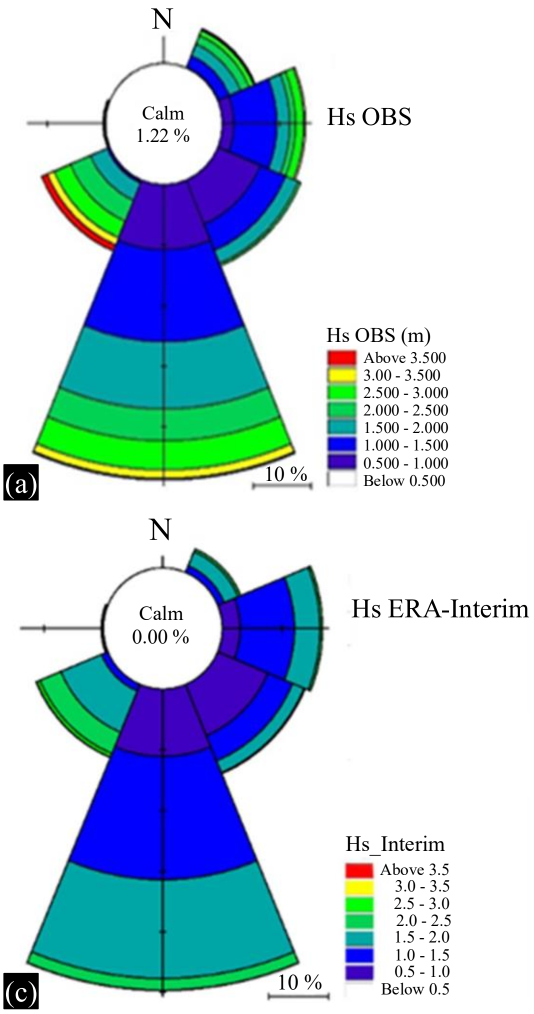

Figure 4. Wave rose diagrams for Joint distribution of Hs and MWD; (a) Buoy, (b) ERA5, and (c) ERA-Interim.

Waves from different ranges of Hs (minimum to maximum) are observed dominantly from the south and to a lesser degree from SW by the Buoy, whereas the models exhibit lower magnitude and standard deviation in Hs. The percentage occurrence of waves from NE is minimal and from the south is maximum, while the rest of the directions show (E, SE, and SW) medium occurrences. Both models underpredicted the peak Hs observed by the buoy, with relatively less deviation from ERA5. The models capture the structure of a variation of Hs well with differences in the percentage occurrences and with less standard deviation as well as directional scatter.

Annual Joint Distribution of Tp and MWD

Wave rose diagrams are plotted based on the joint distribution of Tp and MWD using the Buoy, ERA5, and ERA-Interim datasets, and are compared in Figure 5. Waves from different ranges of Tp, minimum to maximum, were observed predominantly from the south and to a lesser degree from SE and E by the Buoy. The percentage occurrence of waves from NE is minimal and from the south is maximum, while the rest of the directions show (E, SE, and SW) medium occurrences. The ERA5 model overpredicts Tp for the S and SE waves, whereas ERA-Interim overpredicts Tp in the SW direction. The directional distribution is scattered in the models. The models capture the structure of variation of Tp well with differences in the percentage occurrences and with less standard deviation as well as directional scatter.

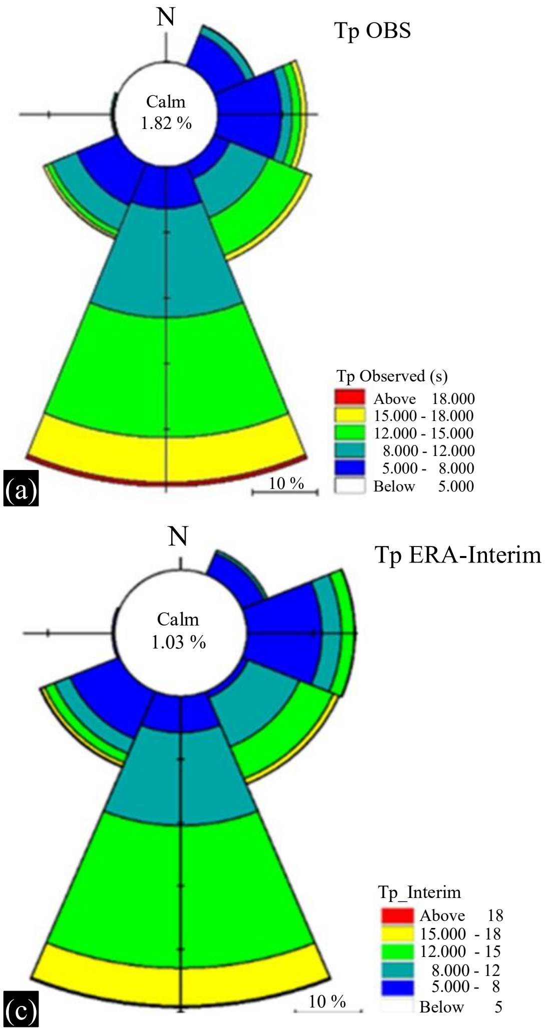

Figure 5. A wave rose diagrams for the joint distribution of Tp and MWD, (a) Buoy, (b) ERA5, and (c) ERA-Interim.

Intra-Annual/Seasonal Variation

The temporal resolution of Hs and Tp for Buoy and ERA5 was 3 h, whereas it was 6 h for the ERA-Interim dataset. Hence, the 6 hourly Observations and ERA5 datasets were derived for consistency and intercomparison.

Monthly Average Hs

The monthly average Hs is inter-compared among the buoy, ERA5, and ERA-Interim, as shown in Figure 6. From January to April, the average Hs from Buoy, ERA5, and ERA-Interim coincided with each other, with average Hs in the range 0.8 of to 1.0 m. During pre-monsoon (May) and post-monsoon (October to December), Hs varied between 1.3 and less than 2.0 m, both models underpredict the Hs with ERA5 having lesser deviation. A similar trend is observed during transition months (August and September), except that Buoy-Hs exhibits Hs of 2.0 m while ERA5 (1.75 m) and ERA-Interim (1.6 m) models underestimate Hs. The peak Buoy-Hs (monthly average) occurred in June (~2.6 m) and July (2.4 m), while both models underpredicted the peak Hs with less deviation for ERA5. ERA5 and ERA-Interim. Both models predicted Hs well and were equivalent to that of the Buoy-Hs from January to April and can be used with confidence. However, both models underestimated Hs from May to December, with mild deviations in the NE monsoon (October to December) and high deviations in the SW monsoon. ERA5, the latest version of the ECMWF, is closer to observations than the previous (older) Reanalysis ERA-Interim.

The monthly Hs of both ERA5 and ERA-Interim coincided with that of Buoy-Hs during the pre-monsoon season (January to April). From May to December, covering SW and NE monsoons as well as the transition periods, both models underpredicted Hs when compared to Buoy-Hs, while ERA5-Hs showed improved skill compared to ERA-Interim-Hs. The peak SW monsoonal waves are highly underestimated by both models, especially ERA5, even after employing state-of-the-art reanalysis. Hence, it is advised not to rely on models for assessing the extreme wave heights during SW monsoons as well as during cyclones, which may be detrimental to estimating the wave power, as well as when considering design aspects such as wave energy conversion (WEC).

Monthly Average Tp

The monthly average Tp is inter-compared among the buoy, ERA5, and ERA-Interim, as shown in Figure 7.

ERA-Interim-Tp

ERA-Interim Tp coincides with Buoy-Tp for seven months during the pre-monsoon (January and March), monsoon (July and August), and post-monsoon (October, November, and December) periods.

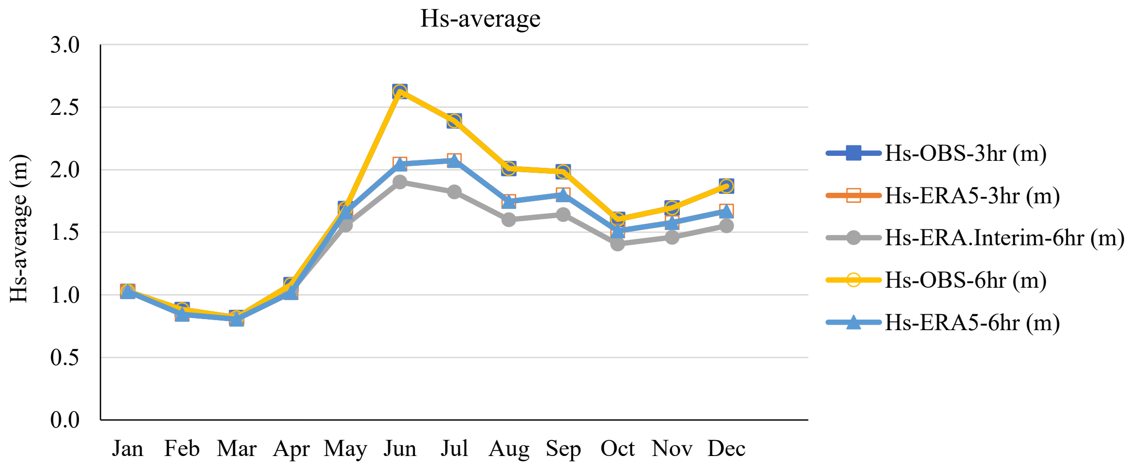

Figure 6. Intercomparison of monthly average Hs from Buoy, ERA5, and ERA-Interim.

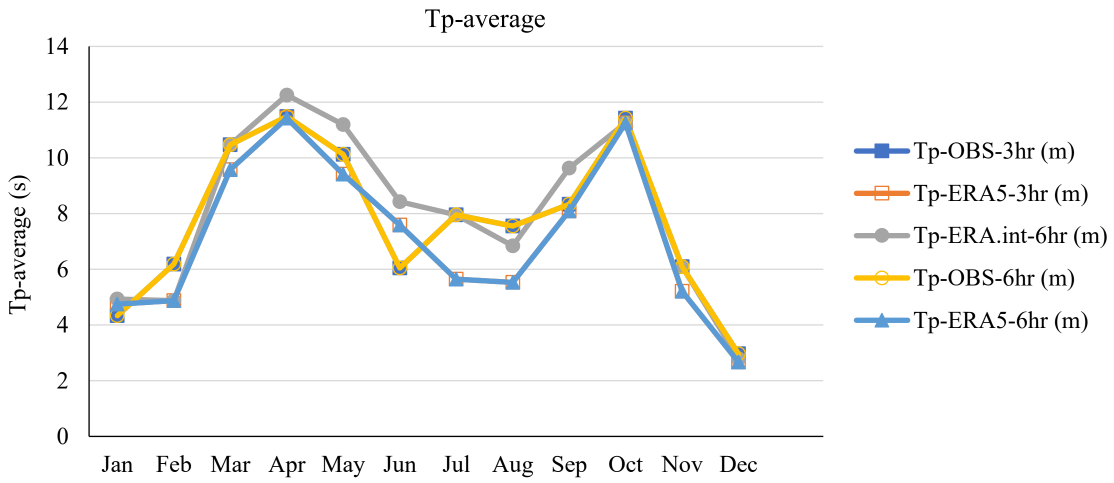

Figure 7. Intercomparison of monthly average Tp from Buoy, ERA5, and ERA-Interim.

Slightly underpredicted Tp (<1.0 s) during February and overpredicted Tp during the rest of the months (April, May, June, and September); with close to 1.0 s deviation during the transition months (May and Sep) and with maximum deviation of 1.5 s during peak Southwest Monsoon (SWM) month in June. ERA-Interim underpredicts Tp during February, March, and August, while the rest of the months it overpredicts. The deviation during the NE monsoon was less than that during the SW monsoon. Tp is high during April and October when the SIO swells reach the Bay of Bengal.

ERA-Tp

ERA5-Tp coincides with Buoy-Tp during the pre-monsoon (January and April) and post-monsoon (September, October, November, and December) periods, while, with less than 0.5 s deviation during March and May. Close to 1.0 s deviation during February (underestimation) and June (overestimation). A maximum deviation of 1.5 s was observed during the SW monsoon months of July and August. The ERA5-Tp deviation during July to August was almost twice that of the deviation during February to March. ERA5-Tp, in general, coincides with Buoy-Tp during low-wave activity (pre- and post-monsoon) or highly underestimated Tp during high-wave activity, such as the SW monsoon. June is the only exception where ERA5-Tp is overestimated compared to Buoy-Tp.

ERA5 versus ERA-Interim-Tp

During the transition months (May and September), ERA-Interim was overpredicted and ERA5 underpredicted Tp by less than 1.0 s. During the SW monsoon (July and August), ERA-Interim almost coincided with Buoy-Tp, while ERA5 underperformed compared to its predecessor with a maximum deviation of up to 1.5 s. June month with peak wave activity is the only exception where both models overpredicted Tp than that of Buoy with ERA5 being the better one with less deviation. Tp is at a minimum during the SW monsoon (JJA), where the local sea wave activity is high. The lowest Tp was observed during December (around 7.5 s) and January (around 8.5 s), where the predictions from both models closely matched the observations. Both models show similar performance and underpredict Tp when compared with the measured one. The maximum deviation between the buoy and model (ERA5) was observed during July and August when the ERA5 deviation was higher than that of ERA-Interim. From April to June, ERA-Interim highly overpredicts Tp in increasing order. July and August months (local wind effect maximum) ERA-Interim shows better performance than September, which is a transition month from the SW to the NE monsoon. Overall, ERA-Interim performed well when local wind waves were dominant and exhibited large deviations when SIO swells contributed at the buoy site. ERA-Interim underpredicted low-wave activity during the calm period and was overpredicted when swells dominated and were closely predicted during the SW monsoon with high-wind seas.

Journal of Remote Sensing & GIS
Volume 16, Issue 1
ISSN: 2230-7990 (Online), ISSN: 2321-421X (Print)

Model Performance

The model performance was assessed by comparing the model parameters with the corresponding buoy-derived parameters using statistical analysis. The statistical parameters used for comparison were the correlation coefficient (r), root-mean-square error (RMSE), bias, and scattering index (SI), which are defined below.

$$r = \frac{N\sum_{i=1}^{N} M_i B_i - \sum_{i=1}^{N} M_i \sum_{i=1}^{N} B_i}{\sqrt{\left[N\sum_{i=1}^{N} M_i^2 - \left(\sum_{i=1}^{N} M_i\right)^2\right]}\sqrt{\left[N\sum_{i=1}^{N} B_i^2 - \left(\sum_{i=1}^{N} B_i\right)^2\right]}} \quad (1)$$

$$RMSE = \sqrt{\frac{1}{N}\sum_{i=1}^{N}(M_i - B_i)^2} \quad (2)$$

$$Bias = \sqrt{\frac{1}{N}\sum_{i=1}^{N}(M_i - B_i)} \quad (3)$$

$$SI = \frac{\sqrt{\frac{1}{N}\sum_{i=1}^{N}[(M_i - \bar{M}) - (B_i - \bar{B})]^2}}{\bar{B}} \quad (4)$$

Where, M_i represents the data obtained from the model (ERA5 or ERA-Interim), B_i represents the data from the buoy measurements, N is the number of data points, and the overbar represents the mean value. The correlation coefficient r represents the trend or pattern followed by the model in relation to the buoy, with a value ranging from -1 to 1 that represents out-of-phase to completely in-phase, respectively. RMSE is a measure of the error or deviation between the model and observations, and a lower value of RMSE indicates a better fit of data between the model and observations. Bias is a statistical quantity that signifies the average difference between model and buoy data. The scatter Index (SI) represents the percentage of RMS difference with respect to the mean observation, or it gives the percentage of expected error for the parameter. The Scatter Index is a normalized measure of error that is often reported as a percentage. Lower SI values indicate better model performance.

Annual Model Performance

The scatter diagrams for Hs between (Buoy versus ERA5) as well as (Buoy versus ERA-Interim) are depicted in Figure 8.

The scatter diagrams for Tp between Buoy versus ERA5 and Buoy versus ERA-Interim are depicted in Figure 9.

The results of the statistical analysis of ERA5 and ERA-Interim with respect to buoy observations are provided in Table 3, considering the entire 2005 period.

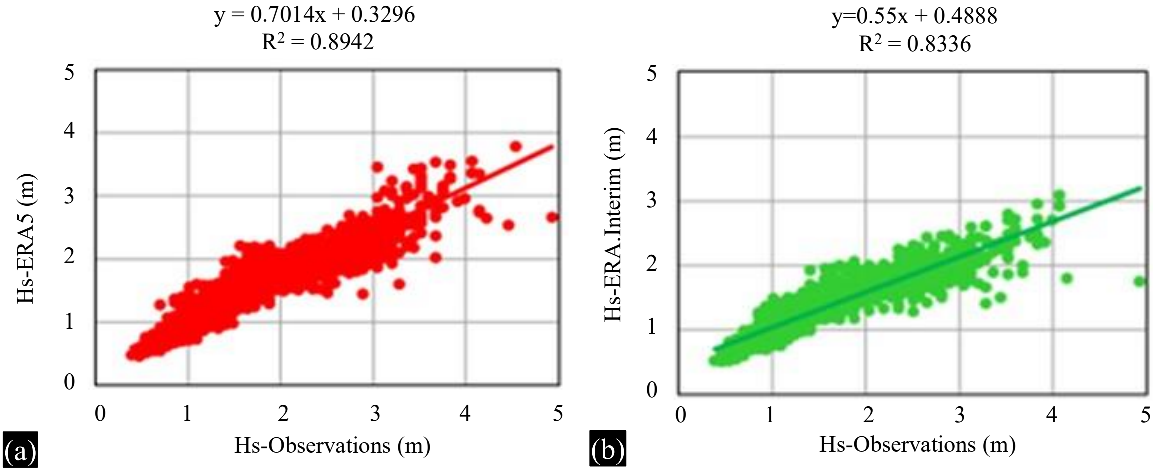

Figure 8. Scatter diagrams for Hs; (a) Buoy versus ERA5; (b) Buoy versus ERA-Interim.

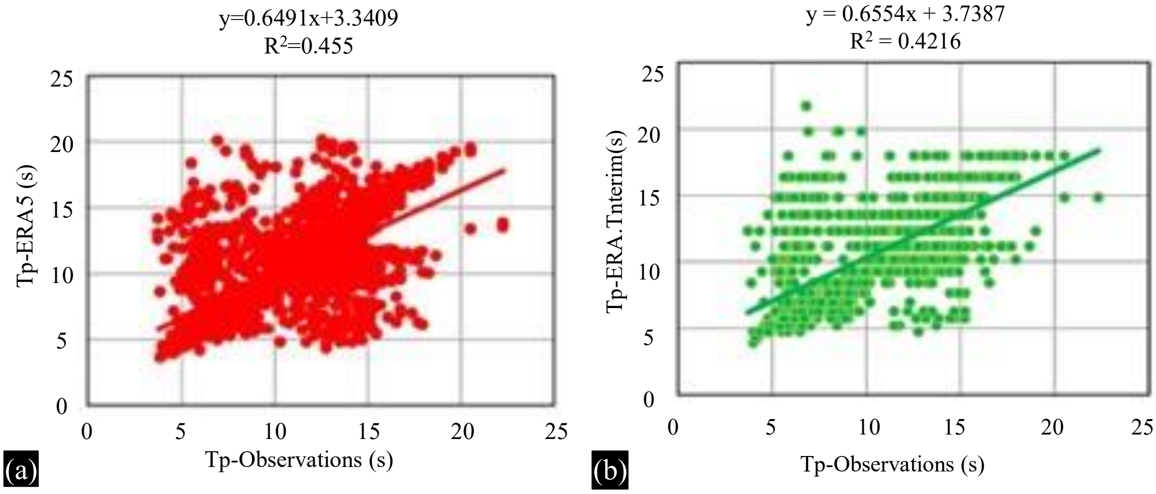

Figure 9. Scatter diagrams for Tp; (a) Buoy versus ERA5; (b) Buoy versus ERA-Interim.

Table 3. Annual statistical analysis of Hs and Tp (Model versus Buoy).

Statistical parameter	Hs			Tp		
	ERA5-3 hrs.	***ERA5-6 hrs.***	***ERA. Int 6 hrs.***	***ERA5 3 hrs.***	***ERA5-6 hrs.***	***ERA. Int 6hrs.***
R	0.9456	0.9460	0.9129	0.6745	0.6771	0.6495
RMSE	0.3241	0.3224	0.4493	2.7322	2.7312	2.8998
Bias	-0.3895	-0.3893	-0.4862	-0.5587	-0.5647	0.3797
SI	0.1777	0.1766	0.2371	0.2607	0.2600	0.2776

r, correlation coefficient; RMSE, root-mean-square error; SI, scattering index

Table 3 reveals that the improvement in the Hs-correlation for ERA5 over ERA-Interim (with respect to observations) is only 3.5%, while the Hs-RMSE is reduced by 37.7%. The improvement in the Tp-correlation for ERA5 over ERA-Interim (with respect to observations) was only 3.8%, while the Tp-RMSE was reduced by only 6.1%. This is attributed to the altimeter data assimilation, which improves the Hs magnitude (variance of the Hs spectrum), but not to the wave period.

The statistical analysis between the moored buoy observations and the global model data products ERA5 and ERA-Interim reveals that the correlation for Hs is good and in the range of 0.91 to 0.95; however, in the case of Tp, the correlation coefficient is poor and only 0.65–0.68. The RMSE for Hs was relatively better (0.32 to 0.45 m), but in the case of Tp, the RMSE range was high, varying from 2.7 to 2.9 s.

Monthly Model Performance

Figure 10 depicts the monthly statistics of R, RMSE, Bias, and Scatter Index for Significant Wave Height between the ERA5 and ERA-Interim models and Buoy Observations.

Figure 11 depicts the monthly statistics of R, RMSE, Bias, and Scatter Index for the Peak Wave Period between ERA5 and ERA-Interim models and buoy observations.

The ranges of different statistical indices in Figures 10 and 11 indicate that there is still a wider scope for improvement in the model prediction of Tp, which is the prime indicator of where (which frequency) the peak energy is contained as well as the mode of forcing, whether it is local wind waves or the remote forcing as swells or is in the mixed sea range. As the wave energy is proportional to the square of Hs and proportional to the wave period, any error in Hs will be doubled and the error in period is further multiplied.

ISSN: 2230-7990 (Online), ISSN: 2321-421X (Print)

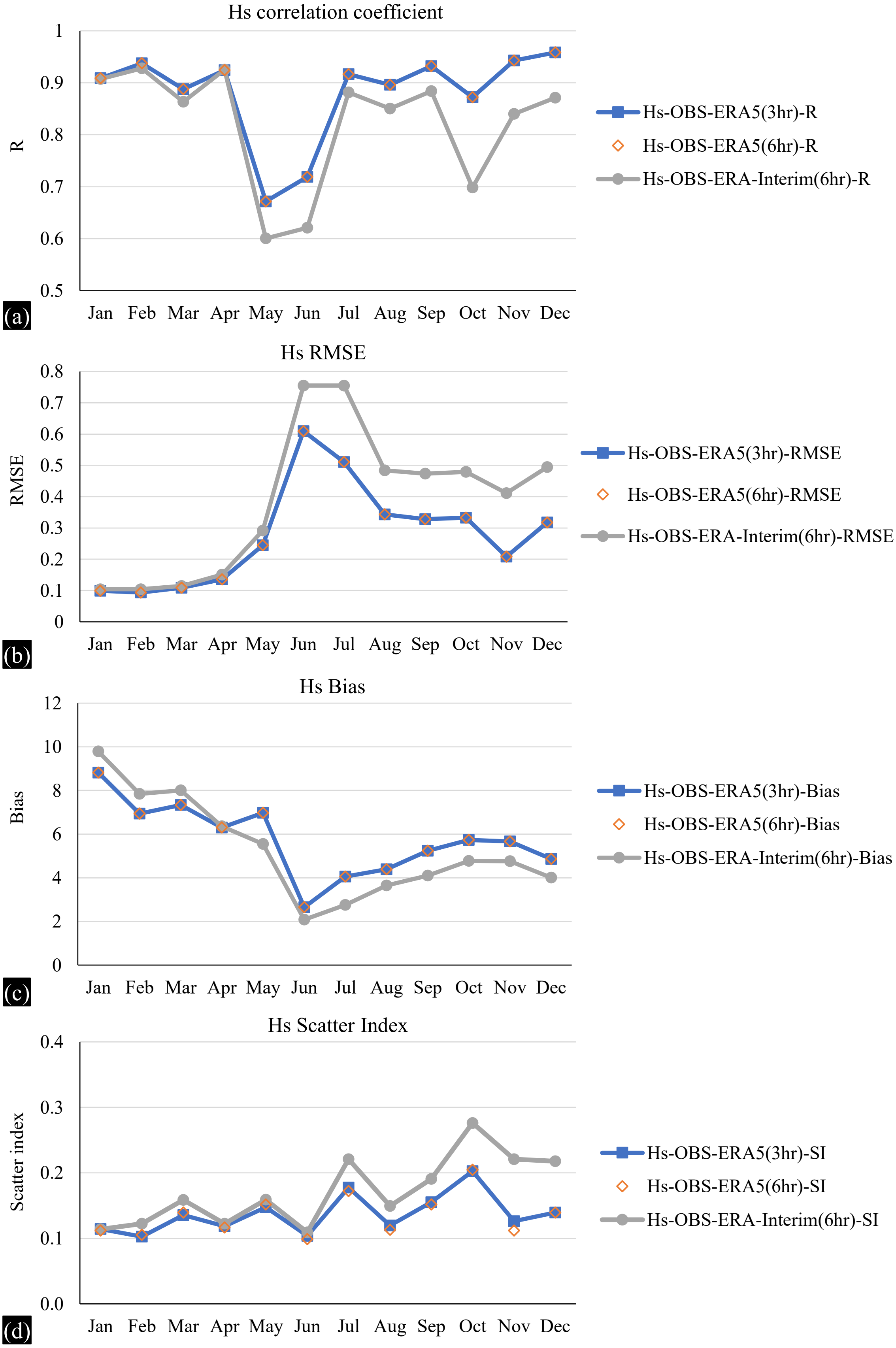

Figure 10. Monthly statistics of R, RMSE, Bias, and scatter index for significant wave height between models and observations.

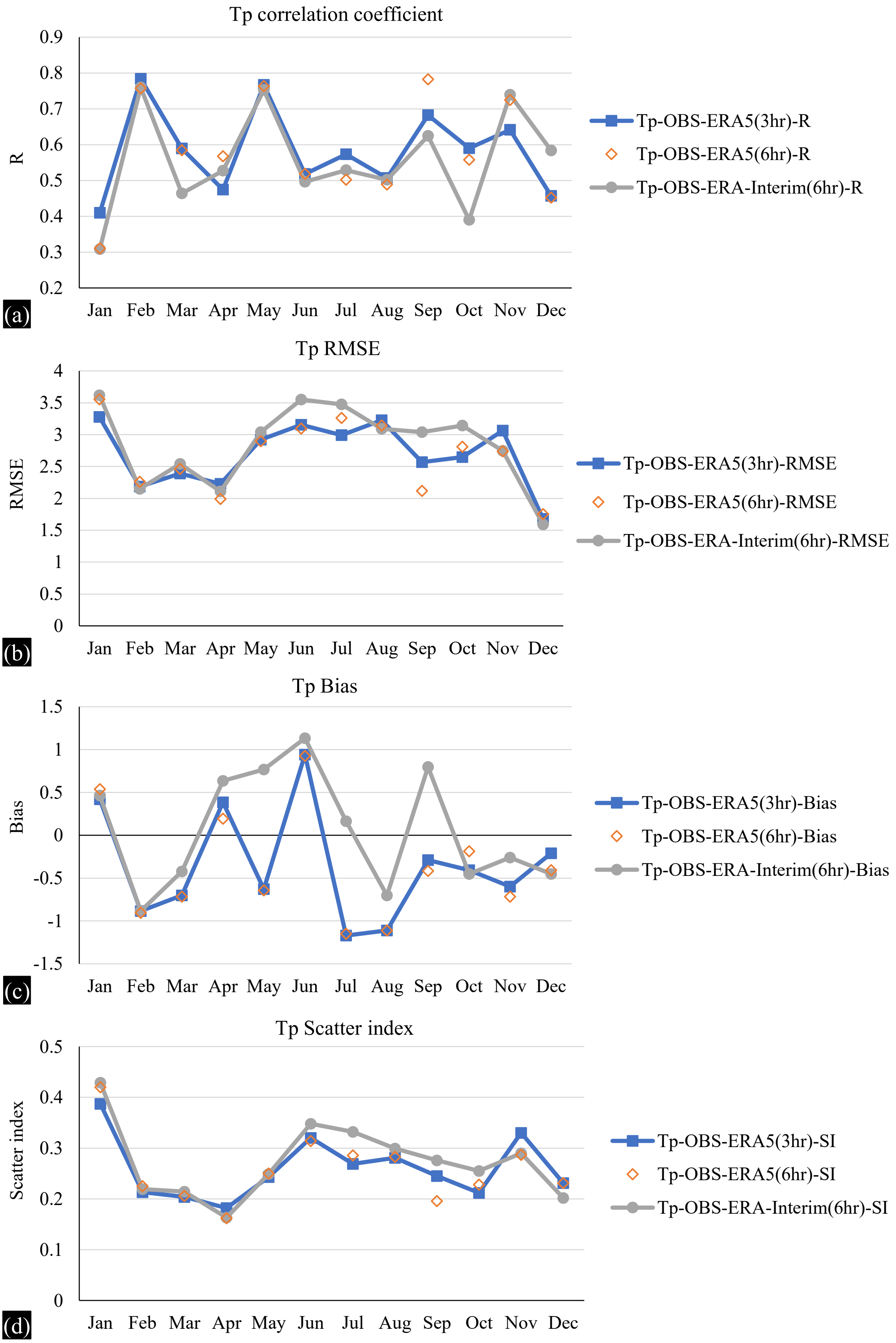

Figure 11. Monthly statistics of R, RMSE, Bias, and Scatter Index for significant wave height between models and observations.

The combined effect of multiple errors in both Hs and Tp can mislead the quantitative assessment of wave energy, particularly during the peak cyclone phase, which will be detrimental to the design considerations of the WEC to withstand the cyclone impact. In addition, a shift in the peak period of approximately 3 s (Δf=0.333 Hz) can change the energy distribution within the wave spectrum and its evolution with respect to time. Moreover, this will misrepresent the nonlinear quadruplet interactions in deepwater at the buoy site as well as the sea-swell interactions, if any, because the energy redistribution within the spectrum is generally centered around the peak frequency (fp=1/Tp).

WAVE PARAMETER RATIOS

To rectify these deviations, moored buoy observations can be utilized as reference measurements, and the wave parameter constants can be derived for Hs and Tp based on their model counterparts (obs/model). These regional constants or WPR will help improve model predictions. These constants are site-specific and model-specific and change with the intensity of wave activity during different seasons as well as based on the performance of the particular model chosen. Hence, it is pertinent to determine seasonally varying constants for each model. In the present study, monthly varying wave parameter ratios (observed/model) were derived using year-long data. To obtain more accurate regional constants, it is suggested to use interannual average wave parameters based on long-term data.

The intercomparison between ERA5 and ERA-Interim monthly averaged Hs-Ratios (wave height ratio; WHR) and Tp-Ratios (wave period ratio; WPR) in the regional waters of NW Bay of Bengal are depicted in Figure 12(a) and (b), respectively.

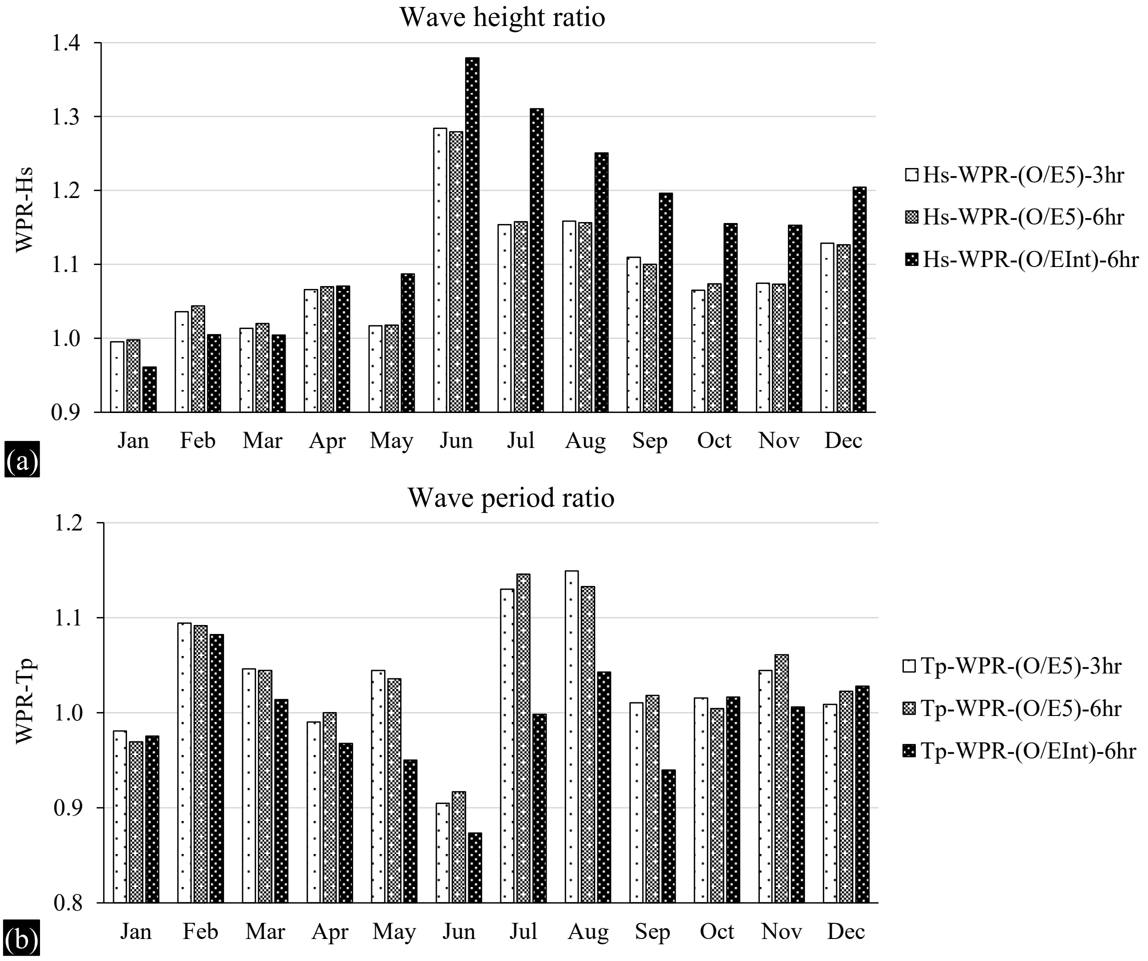

Figure 12. Comparison of (a) monthly Hs-Ratios and (b) monthly Tp-Ratios for ERA5 and ERA-Interim based on buoy observations during 2005.

Effect of Temporal Resolution on WHR (Hs-Ratio)

The effect of temporal resolution (from 3 h to 6 h) on ERA5 Hs-Ratios was not significant, although mild underestimation was observed during the transition months and whenever swells were observed. On the contrary, ERA-Interim (6 h) exhibits low WHR during the pre-monsoon months (January, February, and March) while for the rest of the months during the Monsoon and Post-Monsoon periods, it exhibits high WHR when compared with that of the WHR of the ERA5–6 hr. model. Both almost coincided only for one month (April). Considering the negligible difference in the WHR of ERA5 with temporal resolution, we can deduce that the huge differences in ERA-Interim WHR are due to the different reanalysis products (ERA5 versus ERA-Interim).

Effect of Temporal Resolution on WPR (Tp-Ratio)

The effect of temporal resolution (3 h to 6 h) on ERA5 Tp-ratios (WPR) is visible (though seemingly little) during all months, fluctuating depending on the average Tp for the whole month. It is observed that the WPR of ERA-Interim-6 h is lower than that of ERA5, with a high deviation in the monsoon (June, July, and August) and transition months (May and September). The relative magnitude is the cumulative effect of monsoons, cyclones, and the corresponding sea-swell proportions.

Seasonal Variation of WHR (Hs-Ratio)

The trend in WHR variation was similar for ERA5 and ERA-Interim throughout 2005, except during May, when the WHR of ERA5 decreased from April to May, while that of ERA-Interim increased. From May to December, although the trend was the same as that of ERA5-WHR, ERA-Interim WHR exhibited very high values compared with ERA5-WHR. This is due to the high underestimation of ERA-Interim Hs with respect to that of Buoy (Figure 6) compared to ERA5-Hs, which exhibited better performance owing to its improved version compared to its predecessor, ERA-Interim.

Hs-Ratio varied between 0.95 (January) and approximately 1.4 (June). From Figure 12(a), it is evident that the WHR for ERA5 is less than that for ERA-Interim during the active season (May to December) covering the southwest monsoon and NE monsoons, indicating that ERA5-Hs is relatively close to Buoy-Hs. The difference is more pronounced during the southwest monsoon and post-monsoon months than during the pre-monsoon months, where the ERA5 Hs-ratio is slightly more than that of ERA-Interim (January to March). During April, ERA5 and ERA-Interim performed equally well. ERA-Interim Hs was relatively close to Buoy-Hs during the dry season, exhibiting better prediction during low-wave activity. The highest Hs-Ratios (~1.3 to 1.4) were observed during the SW monsoon months, while the lowest ratios were observed during the dry season (close to 1.0, slight overprediction of low waves by the models).

ERA5-WHR

The WHR (Hs-Ratio) of ERA5 varied from 0.98 (January) to 1.28 (June). During the pre-monsoon (January to May) and post-monsoon (October to November) periods, the WHR of ERA5 is close to 1.0–1.05 predicting close to the Buoy-Hs with only a 5% deviation. September and December show a 10–12% deviation (WHR 1.1 to 1.12), while July and August exhibited a 15% deviation (WHR 1.15). The peak WHR was observed during the SW monsoon in July, close to 1.28, with the highest deviation of approximately 30% for ERA5.

ERA-Interim-WHR

The WHR (Hs-Ratio) of ERA-Interim varied between 0.95 (January) and 1.38 (June) exhibiting a wider range than that of the ERA. During pre-monsoon (January to May), the WHR of ERA-Interim varied between 0.95 (Jan) and equal to Buoy, 1.00 (February and March), and within 10% deviation during April and May. During post-monsoon (September to December) the WHR varied between 1.15 and 2.0 exhibiting 15 to 20% underestimation. In August and July, the WHR varied between 1.25 and 3.0 while the highest WHR of 1.38 happened in June during peak SW monsoon with 38% underestimation.

Impact of Satellite Data Assimilation on Hs-Ratios

This indicates that, during high wave activity, both the ECMWF reanalysis products of ERA5 and ERA-Interim showed the necessity for improvements, though ERA5 to a lesser degree, which is attributed to the ERA5 high temporal and spatial resolution facilitating better representation of cyclones, rapid and short-term changes in wave intensity, improved physics, and 4D-Variational data assimilation utilizing data from the latest satellite altimeter missions.

Seasonal Variation of WPR (Tp-Ratio)

ERA-Interim-WPR

The WPR (Tp-ratio) of ERA-Interim varied between 0.85 (June) and 1.08 (February). The WPR of ERA-Interim is close to 1.0, with less than 5% deviation during January, March, April, May, July, August, September, October, November, and December. During February, the WPR was nearly 1.1 during February, whereas the lowest WPR (0.85 happened during June, which is the peak month of monsoon. ERA-Interim-WPR was minimum in June (0.85) and maximum in February (1.08). During the transition months of May and September, it was approximately 0.95. During July and November, the WPR was 1.00 and equaled the buoy performance. During January and April, it was slightly less than 1.00 and varied between 0.96 and 0.98. In March, October, December, and August, the WPR was slightly higher than 1.00, varied between 1.02 and 1.05 (August). ERA-Interim performed better with its WPR vacillating between 0.95 and 1.05 for 8 out of 12 months, except during the transition months (May and September) and during very calm seas (February), as well as the peak month of monsoon (June). ERA-Interim exhibited a low WPR (higher model-Tp than buoy, leading to low WPR), which leads to underestimation of model-f_p, leading to a shift of the peak towards the (low-frequency band) swell band, that is, the gain of energy or overprediction of wave energy.

ERA5-WPR

The WPR (Tp-ratio) of ERA5 varied between 0.9 (June) and 1.15 (August). Both the maximum and minimum WPR occurred during the SW monsoon months. The WPR of ERA5 is close to 1.0, or within 5% deviation, during the pre-monsoon months (March, April, and May) and post-monsoon months (September, October, November, and December) characterized by low-to-medium wave activity. During January, the WPR was close to 1.0, but slightly underestimated, while the maximum underestimation with a WPR value of approximately 0.9 happened during the peak monsoon (June). An overestimation of 10% (February) to a maximum of 15% (July and August) with WPR varying between 1.1 and 1.15 is found in the case of ERA5. From Figure 12(b), it is evident that the ERA5-WPR is greater than the ERA-Interim-WPR throughout the year, except during January and October, where both performed equally and during December, when the ERA-Interim WPR was slightly higher. The difference is more pronounced during the southwest monsoon months, with a peak difference found during July, followed by August, May, September, June, November, April, March, and February in decreasing order. During October, January, and April, both ERA5 and ERA-Interim performed almost (1.00 to 1.02) equally, vacillating around 1.0 (equal to Buoy-Tp), indicating that the model-Tp matches well with that of buoy-measured Tp. ERA5 performed better with its WPR vacillating between 0.95 and 1.05 for 8 months out of 12 months, except during July and August, which exhibited the highest WPR (1.15) and during very calm seas (February), as well as the peak monsoon month (June). The underestimation of Tp by ERA5 leads to an overestimation of the peak frequency $f_p(=1/Tp)$, leading to a shift of the peak towards the (high-frequency band) wind-sea band, that is, loss of energy or underprediction of wave energy.

The seasonal variation in the wave period ratio reveals that, as the name indicates, it is well suited for predicting/simulating medium-range wave activity. Care must be taken during extreme events where windy seas dominate as well as when remote swells dominate, even during calm sea conditions. The underperformance and lack of consistency during peak wave activity by both models dissuade their use for design purposes with confidence.

CONCLUSIONS

1. *Statistics:* The overall annual statistics, such as correlation coefficient, RMSE, and SI, were improved for ERA5 (3 h and 6 h) compared to ERA-Interim (6 h). ERA-Interim (Tp) exhibited a positive bias, whereas ERA5 (Hs and Tp) and ERA-Interim (Hs) exhibited negative biases.
2. *Hs performance:* The peak SW monsoonal waves are highly underestimated by both models, especially ERA5, even after employing state-of-the-art reanalysis, although their performance is good during pre- and post-monsoons with low-to-medium intensity wave conditions.
3. *Tp performance:* During the transition months (May and September), ERA-Interim overpredicted and ERA5 underpredicted the Tp by less than 1.0 s. During the SW monsoon (July and August), ERA-Interim almost coincided with Buoy-Tp, while ERA5 underperformed compared to its predecessor with a maximum deviation of up to 1.5 s. June month with peak wave activity is the only exception where both models overpredicted Tp than that of Buoy with ERA5 being the better one with less deviation.
4. *Drawbacks of reanalysis models:* The underestimation of Hs during high-intensity waves, as well as inconsistencies with regard to Tp assessment, prohibits these models from relying on them in estimating the design wave parameters for WECs. As the wave power is proportional to Tp and the square of Hs, its estimation using these reanalysis models suffers errors in the manifold (cube) and leads to underestimation or overestimation of the wave energy potential, depending on the case.
5. *Solution using buoy observations:* The use of Indian Constants in the form of WHR and WPR is crucial in alleviating the above-mentioned drawbacks. Based on this study, the model-dependent (ERA5 and ERA-Interim) seasonally varying WHR and WPR can be best utilized to correctly estimate the actual extreme wave conditions (Hs and Tp) during monsoons as well as during different months in a year, and the assessment of wave power as well as the design aspects can be improved for both models. Although the analysis based on one-year data is indicative of the overall structure, it would be more appropriate to use long-term data considering interannual averages if data were available to arrive at seasonally varied WHR and WPR.
6. The variations in the seasonally varying model-dependent wave parameter ratios of Hs and Tp at the buoy site for both ERA5 and ERA-Interim are given below.
   a. *ERA-Interim-WHR:* The WHR of ERA-Interim varied between 0.95 and 1.10 during pre-monsoon (January to May) and 1.15 to 1.2 during post-monsoon (September to December). High WHR is observed during SW monsoon and varies between 1.25 (August) and a maximum value of 1.38 (June).
   b. *ERA5-WHR:* The WHR of ERA5 varied between 1.00 and 1.05 during pre-monsoon (January to May) and 1.05 to 1.10 during post-monsoon (September to December). A high WHR is observed during the SW monsoon and varies between 1.15 (July and August) and a maximum value of 1.28 (June).
   c. *ERA-Interim-WPR:* The lowest WPR of 0.85 (June) happened during the peak monsoon month and the maximum WPR in 1.08 (February) during the calm period. During the rest of the 10 months, the WPR was close to 1.00, with its value vacillating between 0.95 and 1.05.
   d. *ERA5-WPR:* Both the minimum WPR of 0.9 (June) and a maximum of 1.15 (July and August) happened in SW monsoon months, while a value close to 1.1 (February) in a calm period. During the rest of the eight months, the WPR varied between 1.0 and 1.05, except for January, when the value (0.98) was slightly below 1.00.

Acknowledgments

The authors express their sincere gratitude to the Ministry of Earth Sciences for providing an opportunity to work on this project. We sincerely thank Prof. Balaji Ramakrishnan, Director of the National Institute of Ocean Technology, for his support and encouragement in conducting this work. We are indebted to all the staff members of the Ocean Observation Systems Group of the National Institute of Ocean Technology, who are behind the fieldwork for providing the measured data. The ERA5 and ERA-Interim datasets used in this study were obtained from the ECMWF data server (http://data.ecmwf.int/data).

REFERENCES

1. Pogarskii F, Polnikov V, Sannasiraj SA. Joint analysis of the wind and wave-field variability in the Indian Ocean area for 1998–2009. Izvestiya Atmos Ocean Phys. 2012;48:639–56. doi:10.1134/S0001433812060114.
2. Stopa JE, Cheung KF. Intercomparison of wind and wave data from the ECMWF reanalysis interim and the NCEP climate forecast system reanalysis. Ocean Model. 2014;75:65–83. doi:10.1016/j.ocemod.2013.12.006.
3. Sanil Kumar VS, Muhammed Naseef T. Performance of ERA-Interim Wave Data in the Nearshore Waters around India. J Atmos Ocean Technol. 2015;32:1257–69. doi:10.1175/JTECH-D-14-00153.1.
4. Anoop TR, Kumar VS, Shanas PR, Johnson G. Surface wave climatology and its variability in the north Indian Ocean based on ERA-interim reanalysis. J Atmos Ocean Technol. 2015;32:1372–85. doi:10.1175/JTECH-D-14-00212.1.
5. Kumar VS, Joseph J, Amrutha MM, Jena BK, Sivakholundu KM, Dubhashi KK. Seasonal and interannual changes of significant wave height in shelf seas around India during 1998–2012 based on wave hindcast. Ocean Eng. 2018;151:127–40. doi:10.1016/j.oceaneng.2018.01.022.
6. Kumar VS, George J, Joseph D. Hourly maximum individual wave height in the Indian shelf seas—Its spatial and temporal variations in the recent 40 years. Ocean Dyn. 2020;70:1283–302. doi:10.1007/s10236-020-01395-z.
7. Sreelakshmi S, Bhaskaran PK. Wind-generated wave climate variability in the Indian Ocean using ERA-5 dataset. Ocean Eng. 2020;209:107486. doi:10.1016/j.oceaneng.2020.107486.
8. Narasimha Rao TVS, Sundar V. Estimation of wave power potential along the Indian coastline. Ocean Eng. 1982;29:1343–55.
9. Ravindran M, Koola PM. Energy from sea waves – the Indian wave energy program. Curr Sci. 1991;60:676–80.
10. Sannasiraj SA, Sundar V. Assessment of wave energy potential and its harvesting approach along the Indian coast. Renew Energy. 2016;99:398–409. doi:10.1016/j.renene.2016.07.017.
11. Amrutha MM, Sanil Kumar VS. Spatial and temporal variations of wave energy in the nearshore waters of the central west coast of India. Ann Geophys. 2016;34:1197–208. doi:10.5194/angeo-34-1197-2016.
12. Cornett AM. A global wave energy resource assessment. In: Proc Int Offshore Polar Eng Conf. 2008;318–26.
13. Guillou N, Lavidas G, Chapalain G. Wave energy resource assessment for exploitation—A review. J Mar Sci Eng. 2020;8:705. doi:10.3390/jmse8090705.
14. Cahill B. Characteristics of the Wave Energy Resource at the Atlantic Marine Energy Test Site [PhD thesis]. University College Cork; 2013.
15. Cahill B, Lewis T. Wave period ratios and the calculation of wave power. In: Proc 2nd Marine Energy Technology Symposium (METS2014); 2014. Seattle.
16. O'Connell R, de Montera L, Peters JL, Horion S. An updated assessment of Ireland's wave energy resource using satellite data assimilation and a revised wave period ratio. Renew Energy. 2020;160:1431–44. doi:10.1016/j.renene.2020.07.029.
17. Bouttier F, Rabier F. The operational implementation of 4D-var. ECMWF Newsl. 1997;78:2–5.
18. Zuo H, Alonso-Balmaseda M, de Boisseson E, Hirahara S, Chrust M, de Rosnay P. A generic ensemble generation scheme for data assimilation and ocean analysis [Technical Memorandum No. 795]. Reading (UK): ECMWF; 2017. doi:10.21957/cub7mq0i4. Available from: https://www.ecmwf.int/en/elibrary/80380-generic-ensemble-generation-scheme-data-assimilation-and-ocean-analysis.
19. Bengtsson L, Kanamitsu M, Kallberg P, Uppala S. FGGE four-dimensional data assimilation at ECMWF. Bull Am Meteorol Soc. 1982;63(1):29–58. doi:10.1175/1520-0477-63.1.29.
20. Gibson JK, Kållberg P, Uppala S, Hernandez A, Nomura A, Serrano E. ERA-15 Description. ERA ECMWF Re-Analysis Project Report Series. Version 2. Reading (UK): European Centre for Medium-Range Weather Forecasts; 1999.

21. Uppala SM, Kållberg PW, Simmons AJ, et al. The ERA-40 re-analysis. Q J R Meteorol Soc. 2005;131:2961–3012. doi:10.1256/qj.04.176.
22. Dee DP, Uppala SM, Simmons AJ, et al. The ERA-Interim reanalysis: Configuration and performance of the data assimilation system. Q J R Meteorol Soc. 2011;137:553–97. doi:10.1002/qj.828.
23. Hersbach H, Bell B, Berrisford P, et al. The ERA5 global reanalysis. Q J R Meteorol Soc. 2020;146:1999–2049. doi:10.1002/qj.3803.
24. Hersbach H, Dee D. ERA5 reanalysis is in production. ECMWF Newsl. 2016 Spring;(147):7. Available from: https://www.ecmwf.int/en/newsletter/147/news/era5-reanalysis-production.

